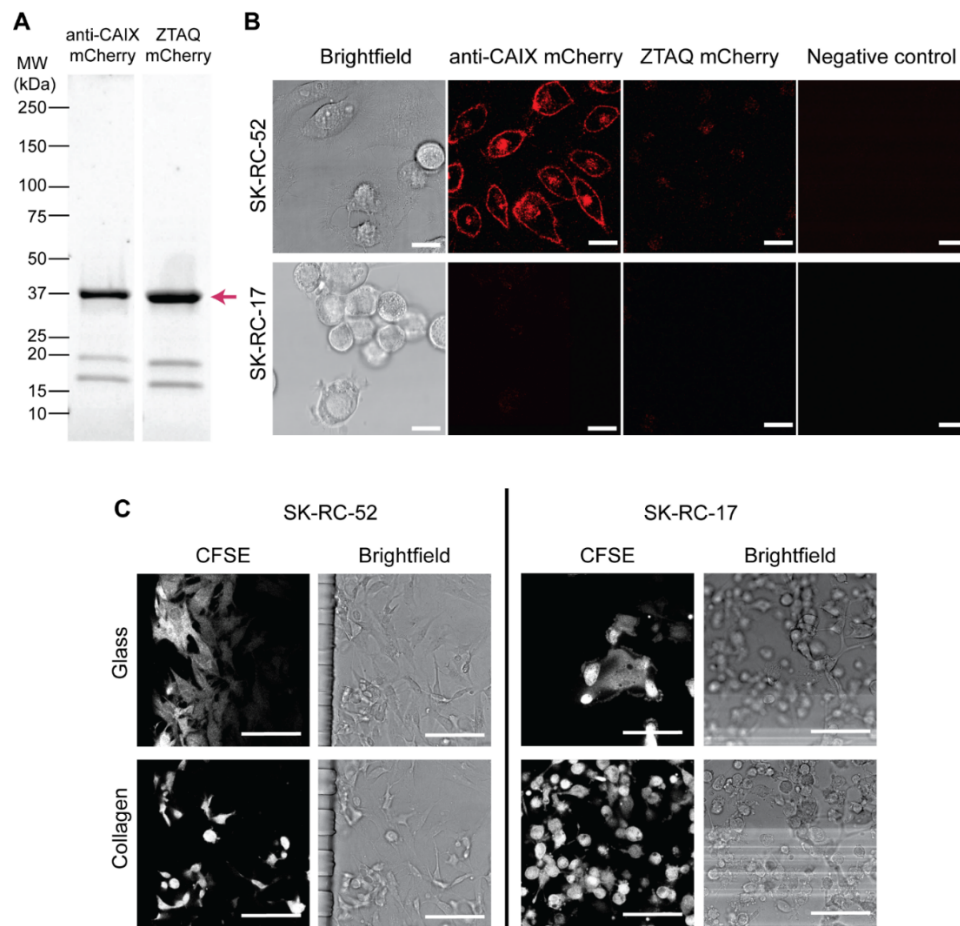


# Supplementary Materials: Mimicking the Biology of Engineered Protein and mRNA Nanoparticle Delivery Using a Versatile Microfluidic Platform

Valentina Palacio-Castañeda, Rik Oude Egberink, Arbaaz Sait, Lea Andrée, Benedetta Maria Sala, Negar Hassani Besheli, Egbert Oosterwijk, Johan Nilvebrant, Sander C. G. Leeuwenburgh, Roland Brock and Wouter P. R. Verdurmen

**Table S1.** Quantitative results of DLS measurements. Averages and standard deviations reflect four repeated measurements. Pdl: polydispersity index.

Sample	Z-Average ( $\text{\AA}$ nm)	Pdl	Attenuator	Intercept	Derived Counts
PF14 + eGFP	80.2 $\pm$ 1.9	0.269 $\pm$ 0.005	8	0.923 $\pm$ 0.001	10,384 $\pm$ 41
LMM + eGFP	525.8 $\pm$ 105.2	0.416 $\pm$ 0.072	8	0.915 $\pm$ 0.003	7448 $\pm$ 1,258



**Figure S1.** Purity and activity of mCherry-affibody fusion proteins in 2D cell culture and morphology of tumor cells in different growth conditions (A) Stain-free SDS-PAGE showing the purified mCherry fusions of CAIX-binding and non-targeting control ZTAQ affibodies, with a size of  $\sim$ 35 kDa. A minor degree of degradation is observed between 15–20 kDa. (B) Confocal microscopy images after a one-hour incubation with the anti-CAIX affibody-mCherry fusion on CAIX-positive SK-RC-52 or CAIX-negative SK-RC-17 cells in 2D, including controls. The brightfield images show the morphology of the cells in 2D cultures. Scale bars represent 20  $\mu\text{m}$ . (C) Confocal images of CAIX-positive SK-RC-52 or CAIX-negative SK-RC-17 cells growing at different heights in the microfluidic device. Scale bars represent 100  $\mu\text{m}$ . CFSE, carboxyfluorescein succinimidyl ester.

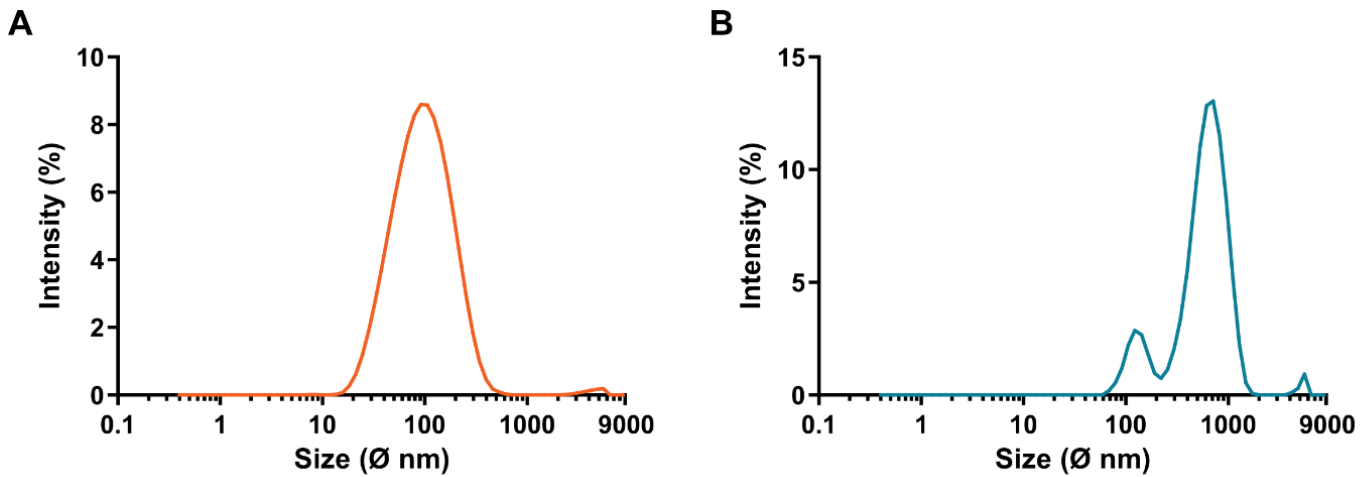


**Figure S2.** Characterization of peptide-based (PF14) and lipid-based (LMM) mRNA transfection complexes. **(A)** Intensity-based particle size distribution of PepFect14 formulated with eGFP mRNA. **(B)** Intensity-based particle size distribution of Lipofectamine MessengerMAX formulated with eGFP mRNA.

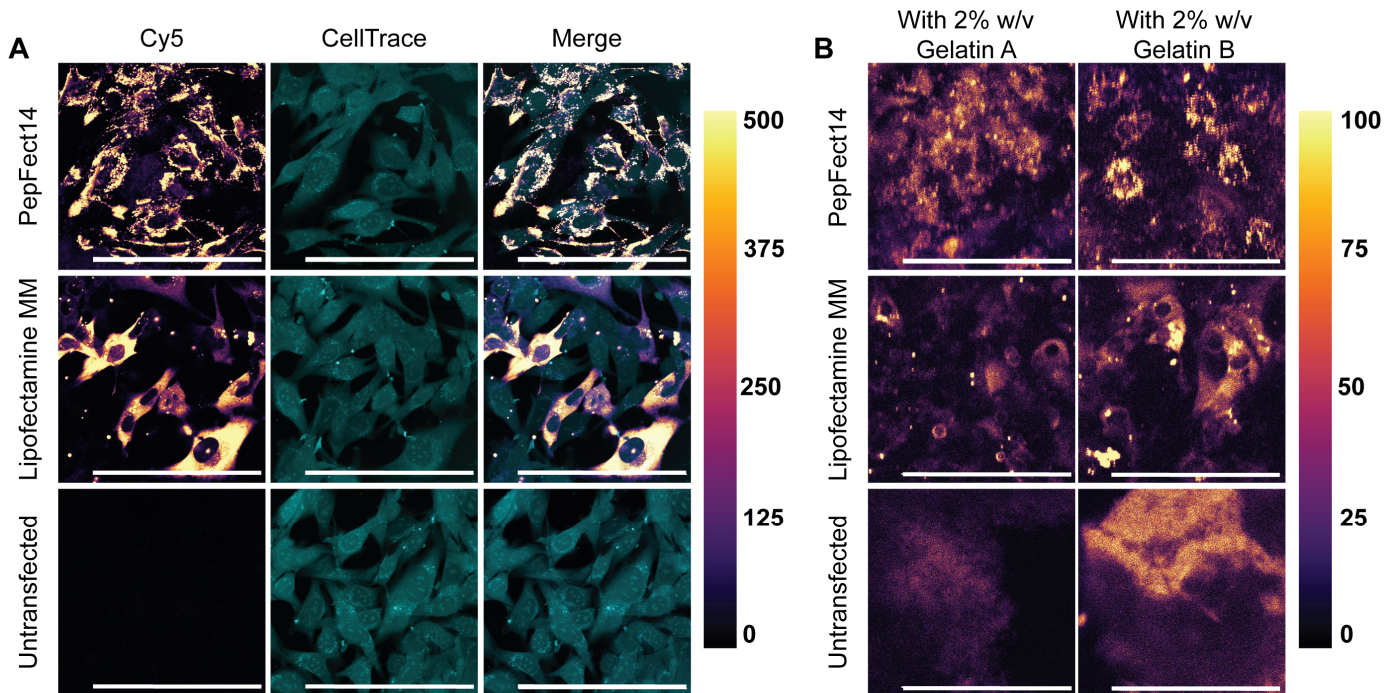


**Figure S3.** Comparison of Cy5-eGFP NP uptake in the presence and absence of colloidal gelatin. **(A)** Uptake of Cy5-eGFP mRNA transfection complexes by MC3T3 cells in Ibidi µ-slide 8 well chambered coverslips (stained with CellTrace Yellow) in the absence of colloidal gelatin. **(B)** Uptake of Cy5-eGFP mRNA transfection complexes by MC3T3 cells seeded in microfluidic chips in the presence of 2% w/v colloidal gelatin. The mpl-inferno LUT depicts the Cy5 intensity, and all Cy5 images were calibrated equally across conditions - per panel - according to the corresponding calibration bar on the right. Scale bars represent 150 µm. Cy5, Cyanine5.

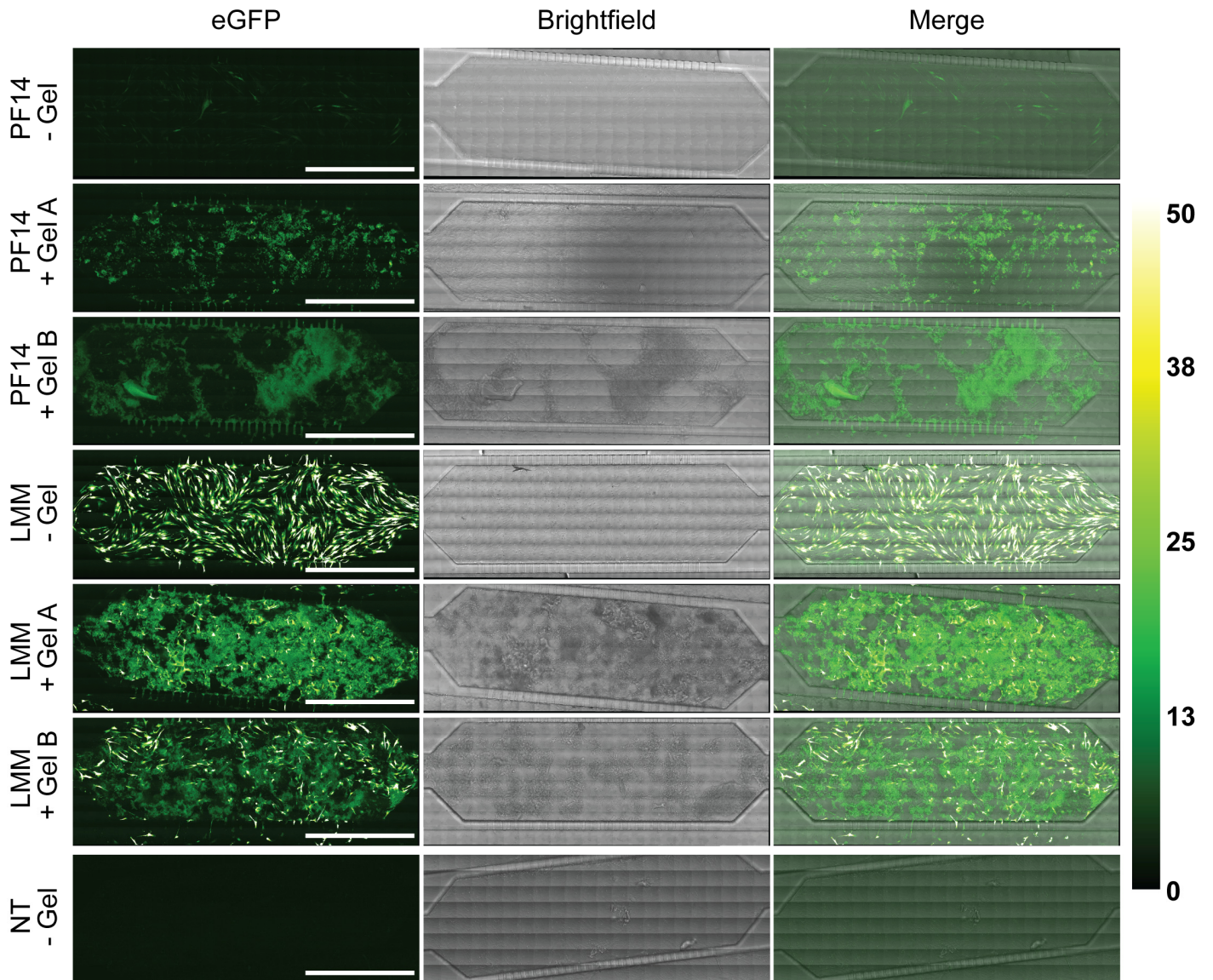


**Figure S4:** Expression of eGFP mRNA in the absence and presence of colloidal gelatin. Confocal microscopy images of MC3T3-associated expression, 24 hours post-transfection. The conditions without gelatin were used to assess the impact of colloidal gelatin on transfection efficiency. The Green-Hot LUT depicts the eGFP intensity, and the brightness and contrast were equally adjusted across conditions according to the corresponding calibration bar on the right. Scale bars represent 1000  $\mu\text{m}$  eGFP, enhanced Green Fluorescent Protein; NT, non-treated.